TWO PHOTON PHYSICS AS AN ATTEMPT TO PROBE PROTON CHARACTERISTICS*

Nikhil Krishna †, Mariola Kłusek-Gawenda

Institute of Nuclear Physics Polish Academy of Sciences
Radzikowskiego 152, 31-342 Kraków, Poland

Received 31 March 2025, accepted 2 April 2025,
published online 26 June 2025

Quantum electrodynamics mechanisms can be used to analyse the proton structure, with particular attention paid to its radius. The cross section for the $\gamma\gamma \to \ell^+\ell^-$ process is placed in the context of proton–proton collisions, allowing for the study of effects related to the distribution of the electromagnetic field around the proton. This research compares the theoretical results with the data from the ATLAS and CMS experiments at the LHC. It allows for the verification of the approach used and the determination of possible model constraints.

DOI:10.5506/APhysPolBSupp.18.5-A17

1. Introduction

Exclusive dilepton production is a fundamental process in high-energy physics. It serves as an important part of the study of quantum electrodynamics (QED) [1], electroweak interactions [2], parton distribution functions (PDF) [3], and potential New Physics beyond the Standard Model (BSM) [4, 5]. Proton–proton collisions studied at energies corresponding to collisions at the LHC provide valuable information about the internal structure, dynamics, and interactions of the proton. Our knowledge has been enriched by information on parton structure, form factors, interactions, and non-perturbative effects.

Since a notable portion of *pp* collisions at the LHC contain quasi-real photon interactions at center-of-mass energies above the electroweak scale, the proton–proton collision at the LHC can be seen as a photon–photon collision. The study of these kinds of interactions in the *pp* collision gives us information about photon content inside the proton and enables the calculation of related cross sections. In this study, we primarily focus on exclusive lepton production processes at the LHC and attempt to probe proton characteristics.

* Presented at the 31[st] Cracow Epiphany Conference on the *Recent LHC Results*, Kraków, Poland, 13–17 January, 2025.

† Corresponding author: `nikhil.krishna@ifj.edu.pl`

2. Radius calculation

The proton charge radius has been measured between 0.841 and 0.877 fm [6] by a number of experimental studies, including electron–proton scattering and spectroscopy methods. The observed differences between various approaches have led to the well-known proton radius puzzle.

The electromagnetic form factors describe the spatial distribution of charge inside the proton. It is possible to consider several types of charge distributions inside the proton and find radius values (Table 1). The information regarding the charge radius can be extracted from the behaviour of the form factor when photons are treated as real (*i.e.*, $Q^2 \to 0$). The nucleon can also be considered as a point-like particle with no internal structure, where the form factor equals unity.

Table 1. Relation between form factors and proton radius for point-like (pl), Gaussian (G), and dipole (D) charge distributions; $\Lambda^2 = 0.71$ GeV^2.

Charge distribution	Form factor	Radius
$\rho(r) = \frac{\delta(r)}{4\pi r^2}$	$F_{\mathrm{pl}}\left(Q^2\right) = 1$	$r = 0$ fm
$\rho(r) = \left(\frac{\Lambda^2}{2\pi}\right)^{3/2} \exp\left(-\frac{\Lambda^2 r^2}{2}\right)$	$F_{\mathrm{G}}\left(Q^2\right) = \exp\left(-\frac{Q^2}{2\Lambda^2}\right)$	$r = 0.404$ fm
$\rho(r) = \frac{\Lambda^3}{8\pi} \exp(-\Lambda r)$	$F_{\mathrm{D}}\left(Q^2\right) = \left(1 + \frac{Q^2}{\Lambda^2}\right)^{-2}$	$r = 0.809$ fm

3. Theoretical overview

3.1. Momentum space approach

The exact calculation of the total cross section for the production of lepton pair in the proton–proton collision, $pp \to pp\ell^+\ell^-$, can be done in the momentum space. In this approach, we introduce full kinematical variables for more precise results. The Feynman diagram presents $2 \to 4$ reaction with four-momenta $p_a + p_b \to p_1 + p_2 + p_3 + p_4$. The general form of the cross section can be expressed by the formula

$$\begin{aligned}\sigma &= \int \frac{1}{2s} \overline{|\mathcal{M}|^2} \, (2\pi)^4 \, \delta^4 \left(p_a + p_b - p_1 - p_2 - p_3 - p_4\right) \\ &\quad \times \frac{\mathrm{d}^3 p_1}{(2\pi)^3 \, 2E_1} \, \frac{\mathrm{d}^3 p_2}{(2\pi)^3 \, 2E_2} \, \frac{\mathrm{d}^3 p_3}{(2\pi)^3 \, 2E_3} \, \frac{\mathrm{d}^3 p_4}{(2\pi)^3 \, 2E_4} \,. \qquad (1)\end{aligned}$$

We extend the integration to eight dimensions to get control over more kinematic ranges. After applying the variable transformations, the final cross section for $2 \to 4$ process becomes

$$\sigma = \int \sum_k \mathcal{J}_k^{-1}\left(p_{1\mathrm{t}},\, \phi_1,\, p_{2\mathrm{t}},\, \phi_2,\, y_3,\, y_4,\, p_{m\mathrm{t}},\, \phi_m\right) \frac{1}{2\sqrt{s\left(s-4m^2\right)}} \overline{\left|\mathcal{M}_{\lambda_3,\lambda_4}\right|^2} \times \frac{1}{(2\pi)^8} \frac{1}{2^4} \left(p_{1\perp}\, \mathrm{d}p_{1\perp}\, \mathrm{d}\phi_1\right) \left(p_{2\perp}\, \mathrm{d}p_{2\perp}\, \mathrm{d}\phi_2\right) \frac{1}{4} \mathrm{d}y_3\, \mathrm{d}y_4\, \mathrm{d}^2 p_{m\mathrm{t}}\,. \tag{2}$$

For photon exchanges considered here, it is convenient to change the variables $p_{1\perp} \to \xi_1 = \log_{10}\left(p_{1\perp}\right)$, $p_{2\perp} \to \xi_2 = \log_{10}\left(p_{2\perp}\right)$. ϕ_1 and ϕ_2 are the azimuthal angles of the outgoing protons, y_3 and y_4 are the rapidities of outgoing leptons, $p_{m\mathrm{t}} = p_{3\perp} - p_{4\perp}$, where $p_{3\perp}$ and $p_{4\perp}$ are the transverse momentum of outgoing leptons. $\phi_{p_{m\mathrm{t}}}$ is the angular orientation of $p_{m\mathrm{t}}$.

The lepton helicity-dependent amplitude for the t-channel, the left diagram in Fig. 1, can be written as

$$\mathcal{M}_{\lambda_3,\lambda_4} = e\, F_{\mathrm{ch}}\left(q_1\right) \left(p_a + p_1\right)^\alpha \frac{-i\, g_{\alpha\mu}}{q_1^2 + i\varepsilon} \bar{u}\left(p_3,\, \lambda_3\right) \gamma^\mu \frac{i\left(\not{p}_3 - \not{q}_1 + m_\ell\right)}{\left(q_1 - p_3\right)^2 - m_\ell^2} \times \gamma^\nu v\left(p_4,\, \lambda_4\right) \frac{-i\, g_{\nu\beta}}{q_2^2 + i\varepsilon} \left(p_b + p_2\right)^\beta\, e\, F_{\mathrm{ch}}\left(q_2\right)\,. \tag{3}$$

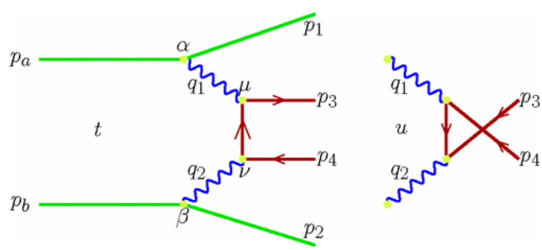

Fig. 1. Exclusive production of di-leptons in pp collision. (Figure from [7].)

Similarly, the amplitude can also be calculated numerically for the u-channel, the right diagram in Fig. 1. The sum of both channel amplitudes is used to evaluate 8-dimensional integration yielding to the total cross section. For both dipole ($F_{\mathrm{ch}} = F_{\mathrm{D}}$) and Gaussian ($F_{\mathrm{ch}} = F_{\mathrm{G}}$) form factors, the total cross section (Table 2) is compared to the experimental findings from the ATLAS and CMS experiments. The theoretical values overestimate the experimental data, but the result considering the proton radius as 0.809 fm is much closer to the measured results. Only the area of a large invariant mass ($M_{\mu^+\mu^-} > 30$ GeV) is not sensitive to details of the proton density, and finally, we get a perfect agreement with ALICE data. Figure 2 shows differential cross section as a function of di-muon invariant mass. The theoretical results preserve the correct shape of contribution. The momentum space approach does not allow for the inclusion of the geometry of the colliding protons. Therefore, it is crucial to consider a model that takes into account the parameter that defines the distance of the colliding nucleons.

Table 2. The total cross section (in pb) for the $pp \to \ell^+\ell^-$ process ($\ell = e, \mu$) at $\sqrt{s_{pp}} = 7$ and 13 TeV. The limit on invariant mass, transverse momentum, and pseudorapidity were defined by the ATLAS (Refs. [8, 9]) and CMS (Ref. [10]) detectors with which the dilepton measurements were performed.

Kinematical constraints	σ_{D}	σ_{G}	σ_{exp}
$pp \to pp\mu^+\mu^-$; $\sqrt{s_{pp}} = 7$ TeV			
$M_{\mu^+\mu^-} > 20$ GeV, $p_{\mathrm{t}} > 10$ GeV	0.70	0.90	0.628 ± 0.038 [8]
$M_{\mu^+\mu^-} > 11.5$ GeV, $p_{\mathrm{t}} > 4$ GeV	4.00	5.15	3.38 ± 0.61 [10]
$pp \to ppe^+e^-$; $\sqrt{s_{pp}} = 7$ TeV			
$M_{e^+e^-} > 24$ GeV, $p_{\mathrm{t}} > 12$ GeV	0.43	0.53	0.428 ± 0.039 [8]
$pp \to pp\mu^+\mu^-$; $\sqrt{s_{pp}} = 13$ TeV			
$M_{\mu^+\mu^-} = (12–30)$ GeV, $p_{\mathrm{t}} > 6$ GeV	2.83	3.47	2.64 ± 0.15 [9]
$M_{\mu^+\mu^-} = (30–70)$ GeV, $p_{\mathrm{t}} > 10$ GeV	0.49	0.59	0.52 ± 0.04 [9]
$M_{\mu^+\mu^-} = (12–70)$ GeV, $p_{\mathrm{t}} > 6$ GeV	4.04	4.25	3.12 ± 0.16 [9]

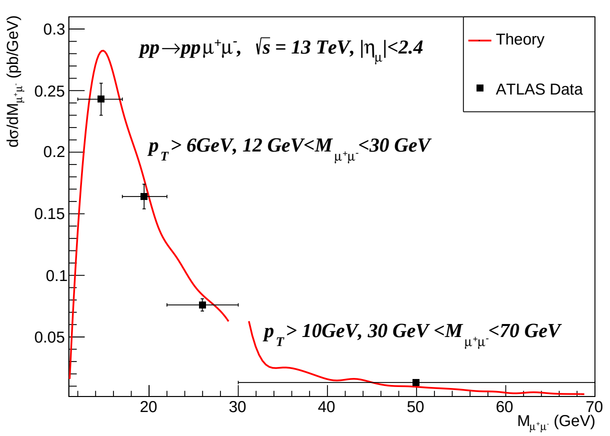

Fig. 2. Differential cross section as a function of the invariant mass of two muons, compared with ATLAS data under two kinematic cuts [9], with each muon detected in $|\eta_\mu| < 2.4$.

3.2. Impact parameter space approach

The Equivalent Photon Approximation (EPA) uses Fermi's formulation, the electromagnetic field of a fast-moving charged particle can be treated as a flux of quasi-real photons [11]. The total cross section for the $pp(\gamma\gamma) \to pp\ell^+\ell^-$ reaction can be approximately described as the photon–photon fusion cross section folded with equivalent photon distributions

$$\sigma\left(pp \to pp\ell^+\ell^-\right) = \int n(\omega_1, b_1)\, n(\omega_2, b_2)\, \sigma_{\gamma\gamma\to l^+l^-}(W_{\gamma\gamma}) \times S^2_{\gamma\gamma}(b)\, b_1\, \mathrm{d}b_1\, \mathrm{d}^2 b_2\, \mathrm{d}\omega_1\, \mathrm{d}\omega_2\, \mathrm{d}\theta\,, \tag{4}$$

where $n(\omega_i, b_i)$ is calculated in terms of photon energy and impact parameter between colliding protons

$$n(\omega, b) = \frac{\alpha}{\pi^2\omega}\left[\int \mathrm{d}q_\perp\, q_\perp^2 \frac{F\left(q_\perp^2 + \frac{\omega^2}{\gamma^2}\right)}{q_\perp^2 + \frac{\omega^2}{\gamma^2}} J_1(bq_\perp)\right]^2 . \tag{5}$$

The impact parameter is expressed through the $\vec{b}_1$ and $\vec{b}_2$ vectors, which mark where the interaction between photons occurs, see Fig. 3.

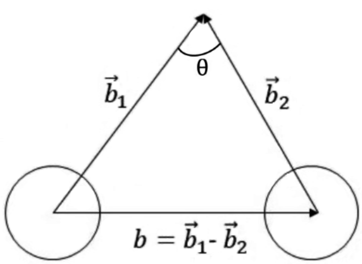

Fig. 3. Schematic view defining the impact parameter space at the collision of protons and accompanying photon fusion.

The ATLAS and CMS collaborations measured cross sections for lepton production for different kinematic regions, which are significantly lower than those predicted by the momentum space approach. One reason for this effect is the finite-size of the proton. The initial step to include the finite-size effect was to introduce a function that represents the probability of not having any interaction between two protons in impact parameter space [12],

$$S^2_{\gamma\gamma}(b) = \left(1 - \mathrm{e}^{\frac{-b^2}{2B}}\right)^2 , \tag{6}$$

where the value of B for 13 TeV is 21 GeV^{-2}, which is an extrapolated value from the ATLAS measurements for the center-of-mass energy of 7 TeV [13].

The total cross section calculated for both point-like and dipole form factors for the $pp \to pp\tau^+\tau^-$ process with and without absorptive effects is shown in Table 3. The higher values of the cross section in p-space are due to the inclusion of an 8-dimensional integration, which covers a broader range of kinematic regions and provides accurate results by including the logarithmic definition of momentum variables. For b-space, we currently use a simplified approach that does not allow for the inclusion of dilepton invariant mass or rapidity range. The problem of considering the smallest values of the impact parameter contributes to the discrepancy between the two approaches. Future calculations in b-space will include additional kinematic variables, which will further improve the accuracy. The inclusion of the absorption factor makes us consider pure QED processes.

Table 3. Total cross sections σ (in pb) for di-tauon production in proton–proton collision at an energy of $\sqrt{s_{pp}} = 13$ TeV calculated for point-like and dipole form factors in the momentum and impact parameter space. The last column includes results with the suppression factor $S^2_{\gamma\gamma}(b)$.

Form factor	$\sigma(p\text{-space})$	$\sigma(b\text{-space})$	$\sigma(b\text{-space}) \times S^2_{\gamma\gamma}(b)$
Point-like	268.34	239.64	229.02
Dipole	178.41	170.21	167.70

4. Summary

The theoretical model introduced in this study incorporates additional kinematic variables in momentum space providing better control over kinematic regions. Our study shows that the dipole form factor reproduces experimental data more accurately, indicating that the charge is distributed exponentially within the proton. We extend our study to impact parameter space, which allows us to examine the proton's absorptive effects using EPA, providing insight into the role of photon flux in exclusive dilepton production processes. The impact parameter framework enables geometrical control over the collision process and allows for precise cuts on kinematic variable, similar to those used at the LHC. This method increases the sensitivity of proton structure measurements by excluding events that are not strictly QED.

This work has been supported by the National Science Center (NCN), Poland, grant DEC-2021/42/E/ST2/00350.

REFERENCES

[1] V. Budnev, I. Ginzburg, G. Meledin, V. Serbo, *Nucl. Phys. B* **63**, 519 (1973).

[2] ATLAS and CMS collaborations (C. Caillol), talk at the 58$^{\mathrm{th}}$ Conference Rencontres de Moriond on Electroweak Interactions and Unified Theories, La Thuile, Italy, 24–31 March, 2024.

[3] G. Chu, J.F. Gunion, *Phys. Rev. D* **10**, 3672 (1974).

[4] ATLAS Collaboration (A. Ogrodnik), *PoS* **(HardProbes2023)**, 067 (2024).

[5] CMS Collaboration (L. Thomas), *PoS* **(DIS2016)**, 111 (2016).

[6] U.D. Jentschura, *J. Phys.: Conf. Ser.* **2391**, 012017 (2022).

[7] M. Kłusek-Gawenda, A. Szczurek, *Phys. Rev. C* **82**, 014904 (2010).

[8] ATLAS Collaboration (G. Aad *et al.*), *Phys. Lett. B* **749**, 242 (2015).

[9] ATLAS Collaboration (M. Aaboud *et al.*), *Phys. Lett. B* **777**, 303 (2018).

[10] CMS Collaboration (S. Chatrchyan *et al.*), *J. High Energy Phys.* **2012**, 052 (2012).

[11] V.M. Budnev, I. Ginzburg, G.V. Meledin, V.G. Serbo, *Phys. Rep.* **15**, 181 (1975).

[12] M. Dyndal, L. Schoeffel, *Phys. Lett. B* **741**, 66 (2015).

[13] ATLAS Collaboration (M. Aaboud *et al.*), *Phys. Lett. B* **761**, 158 (2016).